



Research article

Effect of nordihydroguaiaretic acid cross-linking on fibrillar collagen: *in vitro* evaluation of fibroblast adhesion strength and migration

Ana Y. Rioja ¹, Maritza Muniz-Maisonet ¹, Thomas J. Koob ², and Nathan D. Gallant ^{3,*}

¹ Department of Chemical and Biomedical Engineering, University of South Florida, Tampa, FL 33620, USA

² MiMedx Group, Inc., Marietta, GA 30062, USA

³ Department of Mechanical Engineering, University of South Florida, Tampa, FL 33620, USA

* **Correspondence:** Email: ngallant@usf.edu; Tel: +813-974-5840; Fax: +813-974-3539.

Abstract: Fixation is required to reinforce reconstituted collagen for orthopedic bioprostheses such as tendon or ligament replacements. Previous studies have demonstrated that collagen fibers cross-linked by the biocompatible dicarboxylic acid nordihydroguaiaretic acid (NDGA) have mechanical strength comparable to native tendons. This work focuses on investigating fibroblast behavior on fibrillar and NDGA cross-linked type I collagen to determine if NDGA modulates cell adhesion, morphology, and migration. A spinning disk device that applies a range of hydrodynamic forces under uniform chemical conditions was employed to sensitively quantify cell adhesion strength, and a radial barrier removal assay was used to measure cell migration on films suitable for these quantitative *in vitro* assays. The compaction of collagen films, mediated by the drying and cross-linking fabrication process, suggests a less open organization compared to native fibrillar collagen that likely allowed the collagen to form more inter-chain bonds and chemical links with NDGA polymers. Fibroblasts strongly adhered to and migrated on native and NDGA cross-linked fibrillar collagen; however, NDGA modestly reduced cell spreading, adhesion strength and migration rate. Thus, it is hypothesized that NDGA cross-linking masked some adhesion receptor binding sites either physically, chemically, or both, thereby modulating adhesion and migration. This alteration in the cell-material interface is considered a minimal trade-off for the superior mechanical and compatibility properties of NDGA cross-linked collagen compared to other fixation approaches.

Keywords: collagen; cell adhesion; nordihydroguaiaretic acid; tendon replacement; orthopedic tissue engineering

1. Introduction

Type I collagen is the most abundant protein in the human body by mass, providing the building blocks for tissues such as bones, tendons, dermis, and corneas [1,2]. Thus collagen is frequently used as a candidate resorbable biomaterial for tissue repair or replacement. Tissue-derived collagen molecules reassemble under the proper conditions into native collagen-like fibrils, however the intra- and intermolecular cross-links that form *in vivo* do not occur *in vitro* [2,3,4]. The supramolecular organization of fibrils provides the necessary structural support for tissues and organs, and this spontaneous assembly *in vitro* permits the formation of scaffolds. However, gels formed this way are relatively dilute and fragile, and implantation of reconstituted fibrillar collagen results in rapid degradation and insufficient mechanical support for many applications [2,3]. Therefore, the collagen's mechanical properties must be enhanced in order for this biomaterial to be considered for load bearing applications such as tendon or ligament bioprotheses.

Reconstituted collagen fibrils have been extruded into fibers for tendon and ligament repair or formed into scaffolds for tissue engineering. Typically a fixation step is then required to stabilize the collagen construct and enhance its mechanical properties [2,5]. The fixation strategy is designed to produce a biocompatible and biodegradable biomaterial, with a rate of degradation that is closely tuned to the repair process and the restoration of the desired functional properties in repair tissue. For instance, in the case of reconstituted collagen for orthopedic applications, fixation must also improve the biomechanical performance to provide the required support and maintain its integrity for the extended periods of time necessary for tissue regeneration.

A variety of collagen fixation reagents have been investigated for tissue repair and regeneration including glutaraldehyde, carbodiimides and genipin. Glutaraldehyde, the most common reagent employed to cross-link collagen fibrils, has been extensively studied since it is inexpensive and is capable of rapidly cross-linking via primary amines [2,5,6]. Glutaraldehyde fixed porcine heart valves have been used in humans for many years [7]. However, even though the treatment with glutaraldehyde has been observed to provide stabilization and enhancement of collagen tensile properties, the unreacted residuals and cross-linked products have been shown to be cytotoxic, reducing its acceptability for use in collagen prostheses [8–11]. Unlike glutaraldehyde, cross-linking with carbodiimides do not cause toxicity problems because they are catalytic agents that can be completely washed out of the biomaterial [2,12,13,14]. The carbodiimide compound that is most often used for collagen cross-linking is the water soluble 1-ethyl-3-(3-dimethylaminopropyl) carbodiimide (EDC). EDC induces isopeptide bond formation between carboxylic acid and amine groups on adjacent fibrils [2,15]. Although this cross-linking method produces a collagen product that is more biocompatible than glutaraldehyde, the modest increase in stabilization and tensile properties may not be sufficient for load-bearing tissues [5,16]. Genipin, a natural product from the fruit of the gardenia plant, reacts with free amino groups putatively by forming an aldehyde via ring

opening, and is followed by dimerization [17]. Despite its somewhat similar cross-linking mechanism to glutaraldehyde, genipin fixed tissues are more biocompatible and less cytotoxic [18,19,20]. However, a recent report suggests that the micro- and nano-structure of the collagen is altered by genipin cross-linking [21].

Recently, collagen cross-linked with nordihydroguaiaretic acid (NDGA) has been under investigation for tendon and ligament prosthetics [3,22–26]. NDGA, a naturally derived antioxidant extracted from the creosote bush, is able to cross-link collagen and provide many benefits including stabilization, anti-inflammatory capabilities, and enhanced mechanical properties. The reactive end catechol groups of this antioxidant begin to polymerize when they auto-oxidize, likely forming a network that entraps and reinforces the collagen fibers [3,27]. In addition, the reactive quinones formed by catechol oxidation are also known to bind to lysine and histidine residues on proteins [28,29] which could provide cross-links between the NDGA and collagen polymers. In contrast to glutaraldehyde, NDGA has been shown to perform in a range of clinical applications [3,27,30,31,32]. For example, NDGA-treated type I collagen fibers had tensile properties comparable to those of a human tendon—an average tensile strength of 90 MPa and an elastic modulus of 580 MPa [22]. In comparison, untreated control fibers had tensile strength and elastic modulus of 0.7 MPa and 1.0 MPa, respectively.

Despite the apparent advantages of NDGA fixation for collagen medical products, little is known about how cells interact with this material. Thus, we investigated the effects of NDGA cross-linking on cell adhesion, morphology, and migration; functions that are central to normal wound healing and resorbable biomaterial based tissue repair. Based on previous evidence that NDGA cross-linked collagen supports cell adhesion and proliferation, it was hypothesized that NDGA polymerization would not degrade functional measures of receptor mediated processes including adhesion strength or migration speed. Therefore, the objective of this study was to develop a quantitative *in vitro* platform and investigate cell adhesion and migration on NDGA cross-linked collagen materials that are being developed for tendon and other connective tissue repairs. It was reasoned that if adhesion and migration occurred normally on NDGA cross-linked collagen *in vitro*, then it is expected that, *in vivo*, resident fibroblast and tenocyte cells will be able to populate and remodel a resorbable tendon replacement composed of this material [4]. The results, based on robust hydrodynamic shear force and radial migration assays, indicate that the tradeoffs in cell behavior are minimal for improved mechanical properties, and suggest that further investigation of this biomaterial for use as a tendon or ligament replacement is warranted.

2. Materials and Methods

2.1. Cell culture

Dulbecco's modified Eagle's medium (Invitrogen, Carlsbad, CA) supplemented with 10% newborn calf serum (Invitrogen) and 1% penicillin-streptomycin (Invitrogen) was used as complete growth media (CGM). NIH/3T3 mouse embryonic fibroblasts (American Type Culture Collection, CRL-1658) were cultured in CGM on tissue culture polystyrene. Cells were passaged every other

day and used between passages 5 and 20. For experiments, cells were enzymatically lifted from the culture dish using trypsin/EDTA (Invitrogen) and then homogeneously seeded onto collagen samples by sedimentation.

2.2. Collagen film preparation

Purified pepsin-solubilized type I collagen from fetal bovine tendon (0.5%) in 0.01N hydrochloric acid prepared as described previously [22,24] and provided by MiMedx Group, Inc. (Marietta, GA), was used to fabricate control and NDGA cross-linked collagen films similar to collagen fibers described previously [22,24,25]. The acidic collagen solution was stored at 4°C to prevent gel formation. The working collagen solution was produced by combining the acidic collagen solution with buffered salt solution (pH 7.4), composed of 105 mM NaCl and 53 mM NaH₂PO₄ in deionized (DI) water, in a 1:1 ratio and adjusting the pH to 7.2. Glass coverslips (25 mm in diameter) were sonicated in 50% ethanol, dried under a stream of compressed N₂ and then oxygen plasma cleaned for 5 min (PE50, Plasma Etch, Inc., Carson City, NV). The coverslips were immediately exposed to 0.2% 3-aminopropyl-trimethoxysilane (Gelest) in toluene for 30 minutes, and then immersed in 4% glutaraldehyde in ethanol for an additional 30 minutes. The sequential amine-silane and glutaraldehyde treatments were necessary to provide reactive sites on the supporting glass disks that would covalently anchor the collagen to the surface which was necessary for handling and hydrodynamic shear experiments. These activated surfaces were rinsed with copious amounts of 70% ethanol to remove all unreacted glutaraldehyde, dried under a stream of nitrogen, and placed inside 35 mm polystyrene dishes. 800 µL of the collagen solution was dispensed onto each of the treated coverslips and placed inside a humidified incubator at 37 °C for a minimum of 4 h to ensure the complete formation of fibrillar collagen gels. Collagen gels were then rinsed twice with DI water while rocking for 10 minutes. The gels were allowed to dry overnight at ambient temperature and stored under vacuum for up to 2 days before use. Gels that were completely dried were subsequently called films due to their collapsed structure and reduced thickness. Films were rinsed in 70% ethanol and then rehydrated during the cross-linking procedure or with Dulbecco's phosphate-buffered saline (DPBS, Invitrogen) at the time of use.

2.3. NDGA cross-linking

Collagen films were treated with NDGA as previously described [22,23]; however, some modifications were made since films instead of disks or fibers were being employed. Briefly, NDGA powder (Cayman Chemical Company, Ann Arbor, MI), was dissolved (30 mg/mL) in 0.1 M NaOH, followed by the addition of 0.1 M NaH₂PO₄ (pH 9.0) solution for a final concentration of 3.0 mg/mL NDGA. Dry collagen films were submerged in 2 mL of the NDGA solution and rocked for 24 h to allow complete NDGA polymerization in the presence of ambient oxygen. NDGA-collagen films were rinsed with 0.1 M NaH₂PO₄ solution for 1 h followed by three (20 min) rinses in DI water. Koob et al. previously demonstrated that extensive rinsing eliminated un-reacted intermediates from collagen fibers and made the cross-linking process more effective [22]. The films were then left to

dry overnight. Once cross-linked, the films became opaque and took on the brownish color of the oxidized NDGA solution.

Ultraviolet (UV)-visible absorption spectra of uncross-linked and cross-linked collagen films were recorded with a Synergy HT Multi-Mode Microplate Reader (Biotek Instruments, Inc). The spectra were collected above 300 nm to capture differences unrelated to the strong absorption of tyrosine and phenylalanine residues in the range of 250–300 nm. The results were compared to the measurements completed by researchers at MiMedx Group, Inc. to confirm that the collagen films described herein were cross-linked with NDGA similarly to those previously made in the form of fibers.

2.4. Gel and film thickness measurements

Due to the differences in size scale and physical properties, three techniques were used to measure the thickness of collagen gels and films: side-view imaging, contact profiler, and optical profiler. All three techniques measured the difference (step-change) between the surface of the collagen sample and the supporting glass substrate. The thickness of all the collagen samples, except for the dry films, was determined using calibrated images taken with the side-view camera on a contact angle measurement system (KSV Instruments). The profile image measurements were similar to the expected thicknesses of the gels based on the volume of the collagen utilized divided by the area of the circular cover-slip. For completely dried films, both contact and optical profilers were employed to measure the thickness, which was not detectable by the profile imaging technique. A region of the collagen was removed from each sample so that the height difference could be quantified. A Dektak 150 Surface Profiler (Veeco Instruments, Inc.) with a diamond stylus measured a sample by contacting its surface along a horizontal axis. Line profiles of the vertical displacement were collected and the significant drop from the collagen to the support corresponded to the thickness of the sample. To confirm that the stylus contact did not affect the thickness of the films, a Wyko NT9100 Optical Profiler (Veeco Instruments, Inc.), which calculates the difference in thickness between two surfaces without physically contacting the samples, was also utilized to measure the thickness of the same dry collagen films. The optical profiler yielded a similar average thickness for the collagen films.

2.5. Scanning electron microscopy

The morphology of collagen fibrillar surfaces was examined using a Hitachi SU70 scanning electron microscope (SEM) operated at 10 kV. Briefly, collagen samples were fixed with 3.7% formaldehyde in PBS for 1 hour and then dehydrated. To preserve structure and avoid sample shrinkage, dehydration was achieved in a graded distilled water/ethanol series (30%, 50%, 70%, and 100% ethanol) for 15 minutes each, followed by washes with a graded ethanol/hexamethyl-disilazane (HMDS) series (30%, 50%, 70%, and 100% HMDS) for 15 minutes each [31,33]. The dehydrated collagen samples were sputter-coated with Pd/Au prior to SEM. SEM images were taken at multiple locations across the sample.

2.6. Cytocompatibility

A cell viability assay (LIVE/DEAD, Invitrogen) was performed on adherent cells following the recommended protocol. Fibroblasts were seeded (75 cell/mm^2) on collagen or plain glass control samples and incubated at $37 \text{ }^\circ\text{C}$ for 16 h prior to labeling with calcein AM (labels live cells green) and ethidium homodimer (labels dead cells red). Approximately 3000 cells from 3 samples were analyzed for each surface in 3 independent experiments with a 10X objective. Cell viability was quantified as the ratio of live (green) to live plus dead (red).

2.7. Cell adhesion strength

The spinning disk device was used to quantify the adhesion strength of fibroblasts adhered to collagen samples. This technique applies a linear range of hydrodynamic shear forces for cell detachment under constant and uniform conditions at the surface [34,35,36]. To avoid cell-cell interactions, 50 cells/mm^2 were well dispersed on each sample. After a prescribed time, each sample was mounted on the spinning disk device and spun in DPBS + 2 mM glucose at room temperature for 5 min at a constant speed. After spinning, cells were fixed in 3.7% formaldehyde, followed by permeabilization in 0.5% Triton X-100. These cells were stained with $10 \text{ } \mu\text{g/mL}$ Hoechst 33242 (Invitrogen) and counted at specific radial positions using a Nikon Eclipse Ti-U fluorescent microscope equipped with a motorized stage and NIS-Elements Advanced Research (Nikon Instruments) image analysis software. Using a custom written analysis macro, sixty-one fields were analyzed and cell counts were normalized to the number of cells present at the center of the disk where no shear was applied. The fraction of adherent cells (f) was then fit to a sigmoid curve $f = 1/(1 + \exp[b(\tau - \tau_{50})])$, where the mean adhesion strength (τ_{50}) is the shear stress for 50% detachment and b is the inflection slope.

2.8. Cell spreading and morphology

Fibroblasts were seeded (50 cell/mm^2) on the collagen samples and incubated at $37 \text{ }^\circ\text{C}$ for 4 h. Cells were labeled with $20 \text{ } \mu\text{M}$ CellTracker Green CMFDA (Invitrogen) for 45 minutes. Spreading area and cell shape (circularity = $4\pi \cdot \text{Area}/(\text{Perimeter})^2$) were analyzed using NIS-Elements Advanced Research image analysis software [37,38]. At least four images per sample were acquired and approximately 200 cells were analyzed per sample.

2.9. Cell migration

A circular compartmentalization assay was used to quantify cell migration. The principle of this class of migration assays is based on the release of cells from contact inhibition in a confluent monolayer by removing a barrier [39,40,41]. Sterile substrates were placed in 35 mm polystyrene dishes, and rinsed with DPBS. Polystyrene cloning cylinders (Scienceware, 6.4 mm diameter) were carefully placed on top of the collagen samples. Approximately 33,000 cells were seeded into each

cylinder and incubated at 37 °C for 24 h to allow the formation of a confluent monolayer within the boundary [42]. When the cylinder was removed, each sample was rinsed with DPBS and covered with 2 mL of fresh CGM. The motorized stage of a Nikon Eclipse Ti-U microscope and the image stitching function of NIS-Elements Advanced Research software were used to acquire a 14 by 13 mm compilation picture of the circular monolayer of cells and best fit a circle to the cell population. The samples were replaced in the incubator for 24 h and then imaged again to fit a circle around the cells that were dispersing radially. The average radial migration rate in 24 h was calculated by subtracting the radius of the circle from the image taken 24 h after fence removal minus the radius of the circle from the image taken as soon as the fence was removed from the sample. Migration results were reported as the change in the radius of the circular area covered by cells over the 24 h period ($\mu\text{m}/\text{day}$). Three to five independent experiments were done for each surface.

Mitomycin C was used to block mitosis to investigate the influence of cell proliferation on the increased area coverage of cells on native and NDGA cross-linked collagen films. Mitomycin C is a known inhibitor of cell proliferation which cross-links strands of DNA, thereby inhibiting DNA replication [43,44]. After monolayer formation within circular barriers, 10 $\mu\text{g}/\text{mL}$ Mitomycin C was added to the medium for 1 hour. At the time of cylinder removal, the cells were rinsed with PBS and covered with 2 mL of fresh CGM for the duration of the 24 h migration experiment.

2.10. Statistical analysis

Data are expressed as the mean \pm the standard error of the mean (SEM) of at least three independent experiments ($n \geq 3$). Statistical comparisons for single hypotheses were based on t-tests with a p-value < 0.05 considered significant. For multiple comparisons, analysis of variance and the Holm-Sidak post hoc test were applied with a p-value < 0.05 considered significant. Curve fits of experimental data to specified functions were conducted using the Marquardt-Levenberg algorithm in Sigma-Plot 11 (Systat Software, San Jose, CA).

3. Results

3.1. Collagen substrate fabrication and cross-linking

Type I collagen substrates were prepared by neutralization of the acidic solution and dispensing upon activated glass coverslips followed by drying. Collagen films were subsequently exposed to NDGA which cross-links the collagen and enhances the tensile strength [22,23], thereby restricting the re-swelling of dried films. The use of planar substrates in this study instead of extruded fibers enabled the analysis of morphology of large numbers of cells under uniform chemical conditions and the application of wide ranges of shear stress in the robust measurement of adhesion strength using a hydrodynamic detachment assay.

Visual inspection indicated the conversion of clear collagen samples into dark brown films following exposure to NDGA in the presence of ambient oxygen (Figure 1). In addition, broad

spectrum absorbance was measured on native and NDGA cross-linked samples. NDGA cross-linking was confirmed by enhanced UV-visible light absorbance, and specifically the appearance of a pronounced shoulder at approximately 420 nm. Similar shifts in absorbance around 420 nm following NDGA treatment were observed independently in our lab and for collagen fiber-based products manufactured by MiMedx Group, Inc. This increased absorbance indicates the incorporation of quinones into the collagen films resulting from oxidation of the catechols [45,46].

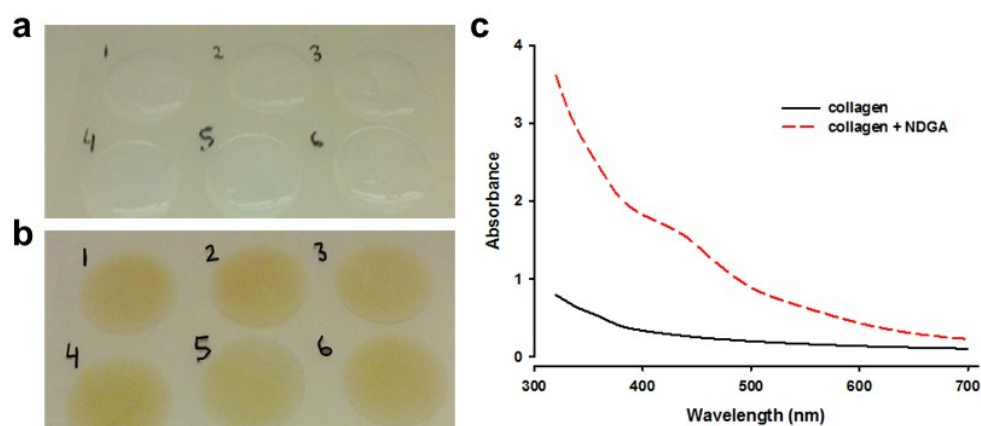


Figure 1. (a) Type I collagen becomes, (b) discolored when cross-linked with NDGA, and (c) UV-visible absorbance spectra of native fibrillar and NDGA cross-linked type I collagen characterizes the change in composition.

The different methods of processing the collagen strongly influenced the final thickness of the samples on which cells were seeded (Table 1). The average thickness of the as-formed collagen hydrogels was approximately $1810 \pm 95 \mu\text{m}$. Upon drying and re-hydrating, which caused collapse ($4.50 \pm 0.52 \mu\text{m}$) and partial recovery ($262 \pm 44 \mu\text{m}$), respectively, an 86% thickness reduction was observed. This drop in thickness was not surprising since approximately 90% of the collagen volume was reduced due to water loss [change in weight before (gel) and after the drying process (film)]. Cross-linking the films during re-hydration was found to cause an even greater reduction in final film thickness (97%) to approximately $63 \mu\text{m}$. By comparison, NDGA fibers manufactured by MiMedx Inc. were found to rebound approximately 60% in diameter after they had been cross-linked and re-hydrated twice. The difference in the extent of recovery volume was likely due to the geometry of the sample. Fibers have a greater surface area to volume ratio and are able to increase in volume in all radial directions; on the other hand, films are confined on one side and only able to increase their volume in a single direction.

Table 1. Collagen sample thickness.

Collagen preparation	Thickness (μm)	Std. Err. (μm)
Gel	1810	95
Film dry	4.50	0.52
Film re-hydrated	262	44
NDGA film re-hydrated	62.6	5.2

Changes in the fibrillar structure attributed to the drying and re-hydration of collagen gels were observed (Figure 2). The as-formed collagen gels had an open, overlapping architecture, while drying and re-hydration resulted in a film with fibrils that were more closely spaced consistent with the incomplete recovery of the original gel thickness. NDGA cross-linked films appeared to be monolithic with decreased void spaces between fibrils. Only native fibrillar or NDGA cross-linked films of type I collagen that had been dried and re-hydrated were used to investigate cell adhesion strength, morphology and migration.

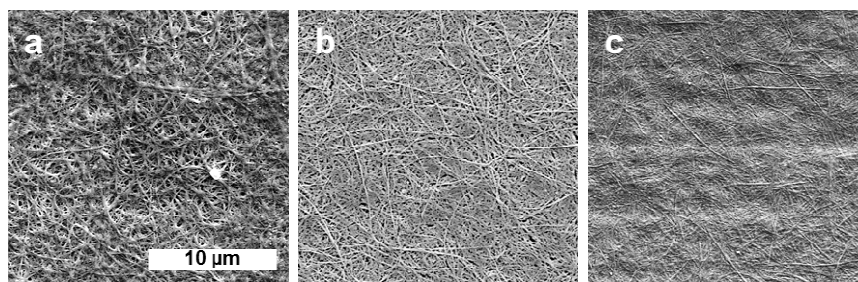


Figure 2. Electron micrographs of (a) a collagen gel, (b) a rehydrated collagen film and (c) a NDGA cross-linked rehydrated film. Scale bar 10 μm .

3.2. Cytocompatibility of NDGA cross-linked collagen

While NDGA cross-linked collagen has been shown to be biocompatible [24], the preparation of the films utilized here required additional fabrication steps to secure them to glass supports for the adhesion assay. Therefore, cell attachment and viability were assessed on native and NDGA cross-linked fibrillar collagen. No significant differences were observed ($p = 0.281$) in mean cell attachment density, which ranged from 73–83 cells/ mm^2 , on collagen and glass control surfaces. Based on a LIVE/DEAD assay, approximately 98% of cells were viable at 16 h with no differences ($p = 0.203$) between collagen preparations and cells attached to glass controls (Figure 3).

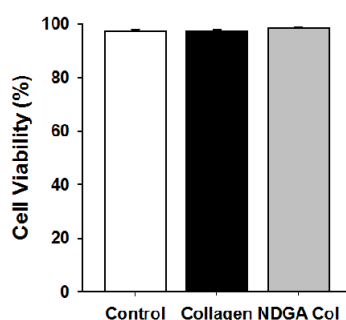


Figure 3. Cytocompatibility was assessed as the percentage of live cells after 16 h adhered to fibrillar collagen substrates. No significant differences were observed between native fibrillar collagen, NDGA cross-linked collagen, and glass controls ($p = 0.203$).

3.3. Cell adhesion strength

The primary goal of this study was the evaluation of effects of NDGA cross-linking on initial cell-collagen adhesion interactions. Cell adhesion strength on native fibrillar and cross-linked collagen films was determined using a spinning disk device, which applies a linear range of forces for detachment under constant and uniform chemical conditions at the surface [34,35,36]. Previous studies found that fibroblasts reach steady-state adhesion strength levels on fibronectin-coated surfaces after approximately 4 h of attachment [35]. Therefore, to determine the time necessary for cells to reach steady-state adhesion strength on collagen substrates, the kinetics of cell adhesion strengthening were established by quantification over 24 h (Figure 4a). A rapid increase in adhesion strength was observed over the first 4 h before steady-state was reached for cells on native fibrillar collagen at approximately 4 h. The experimental data was described accurately by a simple exponential curve and no statistically significant difference ($p = 0.087$) was found between the adhesion strength at 4h (554 ± 23 dyne/cm²) and 24 h (503 ± 14 dyne/cm²). In comparison, at 1 h, the adhesion strength (249 ± 36 dyne/cm²) was observed to be lower than at 4 h ($p < 0.001$), demonstrating that adhesion strength increased up to 4 h. Based on these results, steady-state (4 h) adhesion strength was quantified on native fibrillar and cross-linked collagen films. A small ($\sim 18\%$), but statistically significant decrease ($p < 0.05$) in mean adhesion strength was observed on NDGA cross-linked collagen (456 ± 35 dyne/cm²) in comparison to native collagen (554 ± 23 dyne/cm²) show in Figure 4b.

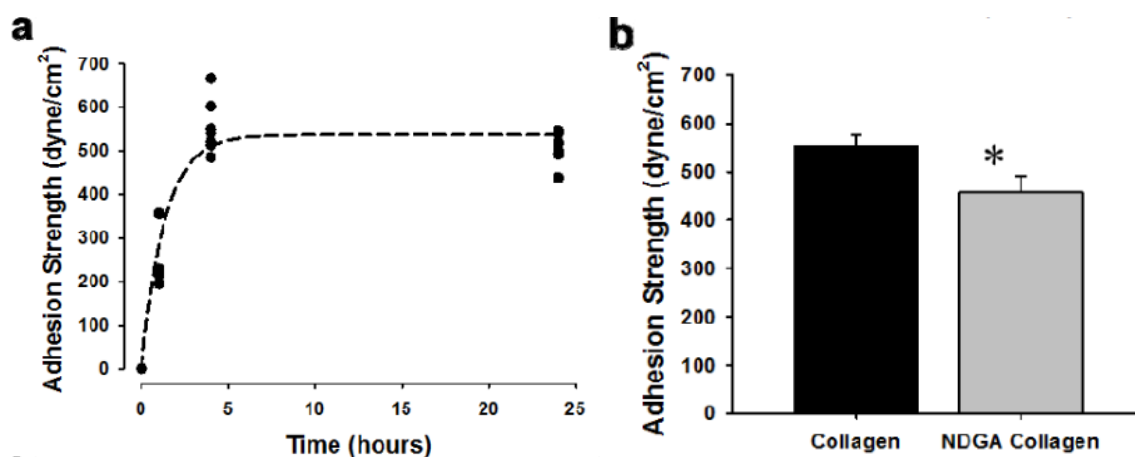


Figure 4. Adhesion strength of NIH/3T3 embryonic fibroblasts on reconstituted collagen was quantified using hydrodynamic shear. (a) Temporal evolution of mean cell adhesion strength (τ_{50}) on native fibrillar collagen exhibited rapid increases until reaching steady-state values at 4 h. An exponential curve accurately described the data ($R^2 = 0.86$). (b) Mean cell adhesion strength on native fibrillar and NDGA cross-linked type I collagen at steady-state (4 h). An asterisk denotes a statistically significant difference between the groups (*t-test: $p < 0.05$).

3.4. Cell spreading and morphology

Cells were fluorescently labeled with CellTracker CMFDA and fixed in order to analyze spreading and circularity on native fibrillar and NDGA cross-linked collagen films (Figure 5). There was no significant difference in projected cell area between cells on collagen films after 4 and 24 h (*not shown*), indicating that cell spreading reached steady-state by 4 h and confirming the kinetics of adhesion strengthening. At steady-state adhesion, cells on uncross-linked fibrillar films spread to an average area of $1049 \pm 11 \mu\text{m}^2$, which was significantly greater ($p < 0.005$) than the average spreading area of cells on NDGA cross-linked collagen ($685 \pm 59 \mu\text{m}^2$).

Cell morphology was also characterized by a shape factor known as circularity, which varies from 0 to 1. Circularity values close to 1 signify rounded morphologies, whereas intermediate values indicate a transition toward more stellate or polarized morphologies and values near 0 describe highly branched or elongated shapes. Quantification of cell circularity (Figure 5d) indicated there was a significant increase in circularity ($p < 0.005$) for cells on cross-linked films (0.67 ± 0.02) compared to uncross-linked films (0.52 ± 0.03).

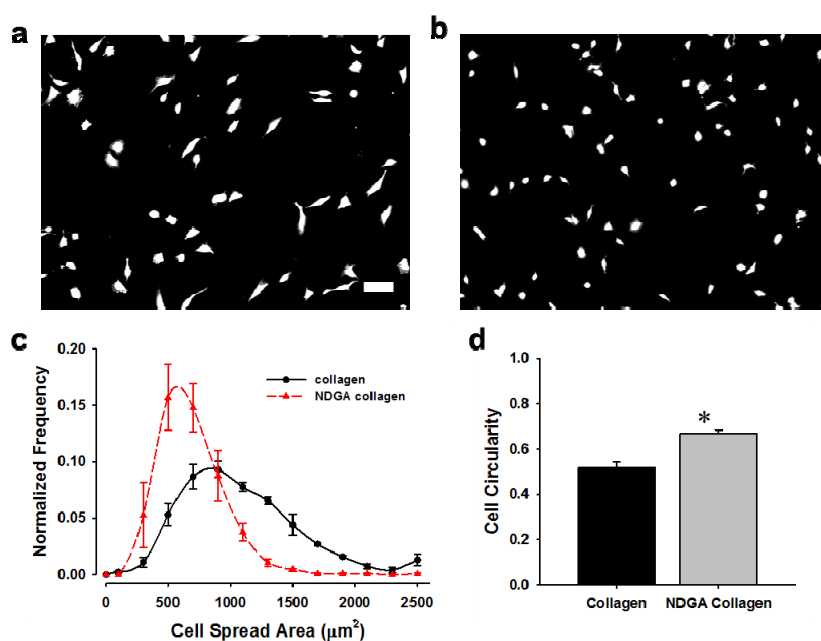


Figure 5. Cell spreading and morphology on native fibrillar and NDGA cross-linked type I collagen. Projected cell area and shape at steady-state were quantified on (a) native fibrillar and (b) NDGA cross-linked type I collagen. Scale bar 100 μm . (c) Histograms of cell area were constructed from binned cell spreading measurements from approximately 200 cells (t-test: $p < 0.005$). (d) Cell shape (circularity = $4\pi \cdot \text{Area} / (\text{Perimeter})^2$) at steady-state for cells attached to native fibrillar and NDGA cross-linked type I collagen. An asterisk denotes a statistically significant difference between the groups (*t-test: $p < 0.005$).

3.5. Cell migration

Migration on collagen materials was investigated by quantifying the rate of radial dispersion of cells from a circular region following the removal of a barrier. The migration rate was analyzed because it is a cell function central to tissue regeneration that is strongly related to cell spreading and adhesion strength. Cell migration rate was quantified as the change in the radius of the circular area covered by cells over the 24 h period after the barrier was removed (Figure 6). The average radial migration of the cells seeded on top of the NDGA cross-linked collagen films ($151 \pm 24 \mu\text{m}/\text{day}$) was found to be significantly lower ($p < 0.001$) than on the uncross-linked samples ($389 \pm 40 \mu\text{m}/\text{day}$). To investigate the influence of cell proliferation on the radial dispersion of cells on native and NDGA cross-linked collagen films, mitomycin C was used to block proliferation. No differences in migration were observed when proliferation was inhibited for either native collagen or NDGA cross-linked collagen films relative to the uninhibited case ($p > 0.34$), which suggests that this metric reflects only radial cell movement over the first 24 h after fence removal.

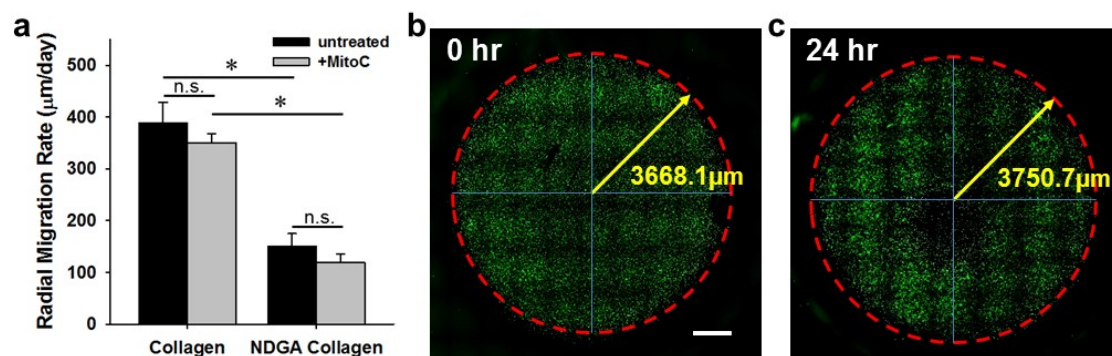


Figure 6. Cell migration on native fibrillar and NDGA cross-linked type I collagen. (a) Migration ($\mu\text{m}/\text{day}$) was quantified as the collective radial dispersion of a confluent monolayer following the removal of a confining boundary (*t-tests: $p < 0.001$; n.s.: not significant, $p > 0.05$). Mitomycin C ($10 \mu\text{g}/\text{mL}$ for 1 h) was added to block proliferation. Representative composite images stitched together from adjacent fields of view at (b) time of fence removal and (c) 24 h later on NDGA cross-linked collagen annotated with measurements (bar = $1000 \mu\text{m}$).

4. Discussion

NDGA cross-linked fibers are biocompatible [24,25] and have tensile properties comparable to those of native tendons [22]. The goal of this study was to investigate the effect of NDGA cross-linking on fibroblast adhesion strength and migration during initial interactions using quantitative *in vitro* assays. The collagen was cast into films to facilitate the rotating disk cell adhesion strength analysis which applies a large range of forces to a large population of cells [35]. Despite the difference in geometry between extruded fibers for tendon replacement and the planar films

described here, the samples were demonstrated to be chemically similar by UV-visible absorbance. However, the process by which these films were formed introduces differences in thickness between native fibrillar collagen and NDGA cross-linked collagen films, presumably because the NDGA cross-linking restricts swelling. Instead of normalizing the final thickness by altering the amount of collagen used to form the initial collagen gels, gels from similar collagen concentrations were used to prepare control and NDGA cross-linked films so that the surface density of cell binding sites would be similar. Thus, a compromise was made between the final thickness and the limitations of the gel fabrication process in order to approximate the size of the fibers that are under commercial development for tendon prostheses. The resulting NDGA cross-linked collagen films were approximately 60 μm thick, which approximates that of the collagen fibers and more importantly is an order of magnitude greater than the accepted depth over which cells can mechanically sense underlying rigid supports through soft gels [47]. This ensured that the scale of the various film thicknesses would not contribute to the observed differences in cell responses. The morphology of the collagen networks was consistent with changes in thickness upon drying and re-hydrating. The observed compaction corresponded to decreased spacing between fibrils.

Once sufficiently thick collagen films were fabricated and NDGA cross-linking was confirmed by the spectral absorbance, *in vitro* assays were performed to determine if initial cell behaviors were modulated by the cross-linking treatment of the collagen samples. A cell viability assay indicated that not only was the NDGA treatment not detrimental to attached cells, but that the glutaraldehyde method of fixing the collagen gels to glass supports was also not cytotoxic for these short duration experiments. Previous adhesion studies have demonstrated that the strengthening kinetics of NIH/3T3 fibroblasts on fibronectin leads to rapid enhancement of adhesion strength upon attachment, with saturation being reached by 4 h after contact [35]. Similar adhesion kinetics was observed for cells on collagen films; therefore, adhesion strength, morphology and migration were analyzed for cells incubated on fibrillar and NDGA cross-linked collagen films for 4 h. To summarize, small but significant reductions in cell adhesion strength, spreading and migration, as well as slightly increased roundness were observed on NDGA cross-linked collagen compared to native fibrillar collagen. One possible explanation for the difference is the increased stiffness caused by cross-linking the collagen fibrils; however, based on previous reports of responses to other materials, the opposite trend would be expected [48,49,50]. A more likely explanation is a decrease in accessible integrin binding sites at the collagen surface due to physical masking during the NDGA polymerization process. Nevertheless, NDGA did not prevent strong cell adhesion and migration on fibrillar collagen.

The mechanism of NDGA interaction with collagen is not completely understood. NDGA treatment of collagen had been considered to be primarily an NDGA polymerization process [3,25,27,32], which physically constrains the fibrillar collagen. However, the reactive quinones that are generated from catechol oxidation have been demonstrated to covalently bind proteins *via* lysine and histidine residues [28,29]. Thus, a secondary mechanism is proposed that depends on the densification of the collagen that occurs when collagen gels dry and collapse into compacted structures (films or fibers). This effectively pushes the collagen fibrils closer together which may promote enhanced interfibril interactions, and could also allow the available shorter links of the NDGA to cross-link to the collagen networks. This cross-linking between the collagen fibrils

within the film and with NDGA may be occurring when the collagen reacts with the NDGA in the compacted structure. Consequently, interfibrillar cross-linking, which does not appear to occur *in vitro* when collagen gels are formed and maintained in a fully hydrated state, may explain the inability of dried fibrillar collagen substrates to fully rebound to the original as-formed thickness. Moreover, it would indicate that the enhanced tensile strength of the material comes from both natural and NDGA cross-links which do not appreciably occur when the collagen self-assembles into gels and the fibrils are highly separated.

Consistent with this mechanism, it is also hypothesized that the small differences observed in cell adhesion, spreading and migration occurred because NDGA cross-linking masked a fraction of the adhesion receptor binding sites either physically, chemically, or both. Adhesion and spreading are not independent; reductions in both can result from decreased ligand density [51–54]. With fewer available binding sites, cells typically exhibit reduced adhesion strength [35,55,56]. Future work will focus on independently examining these chemical and mechanical inputs that regulate cell behavior.

Although adhesion, spreading, and migration were slightly decreased for fibroblasts seeded on top of NDGA cross-linked collagen, the reduction does not preclude this biomaterial from use in tissue repair applications such as a tendon replacement. This is supported by the finding that other common collagen cross-linking approaches such as carbodiimides, which produce lower tensile strength than NDGA, demonstrate that the cell responses such as spreading area are also reduced when cells are seeded on the carbodiimide cross-linked surfaces [57]. This study has established that cells are able to adhere strongly to and migrate on the NDGA cross-linked collagen surfaces, which is necessary for recruitment of resident cells *in vivo* for rapid tendon regeneration. In addition, a recent study showed that cyclic stretching induced stem cell differentiation into fibroblasts on NDGA cross-linked collagen, further supporting that sufficient integrin binding for mechanotransduction does occur [26]. Finally, even though the present investigation was focused on collagen formed into films, it can be inferred that cells will also populate and migrate on NDGA-collagen biomaterials with other geometries including fibers and scaffolds.

5. Conclusions

It has been reported that NDGA possesses numerous advantages including biocompatibility, biodegradability, and organizational enhancement of tensile strength over other cross-linking approaches (e.g. glutaraldehyde, carbodiimide) which have been investigated for augmenting the strength of collagen materials. The results of this study demonstrate that NDGA cross-linking causes small but significant changes in initial cell behavior (cell spreading, migration, and adhesion) on collagen films. The small decreases in adhesion strength and migration caused by NDGA are likely caused by reductions in the available adhesion sites necessary for anchorage by either physical masking (NDGA polymerization), chemical blockage (collagen-collagen and NDGA-collagen cross-linking), or both. However, even though NDGA fixation alters early cell interactions with collagen, this material still supports substantial cell adhesion and migration. Based on these results, it can be concluded that NDGA cross-linked collagen is a promising biomaterial for applications such as tendon or ligament replacement. Further investigation is warranted to understand the mechanisms of

NDGA cross-linking and the role of integrin receptor binding in governing cell interactions with this material.

Acknowledgements

The authors thank Ivan Rivera for assistance with SEM imaging and the USF Nanotechnology Research and Education Center for assistance with film thickness measurements. Funding was provided by the National Science Foundation (CAREER DMR-1056475, S-STEM DUE-0807023). AYR, MMM and NDG disclose that they have no financial interest in the MiMedx Group, Inc. TJK is the Chief Scientific Officer of MiMedx and inventor of the NDGA collagen cross-linking technology.

Conflict of Interest

All authors declare no conflicts of interest in this paper.

References

1. Alberts B (2008) Molecular biology of the cell. New York: Garland Science.
2. Koob TJ (2004) Collagen fixation. *Encyclopedia Biomater Biomed Eng* 1: 335–347.
3. Koob TJ (2002) Biomimetic approaches to tendon repair. *Comp Biochem Physiol A Mol Integr Physiol* 133: 1171–1192.
4. McCarthy JB, Vachhani B, Iida J (1996) Cell adhesion to collagenous matrices. *Biopolymers* 40: 371–381.
5. Rault I, Frei V, Herbage D, et al. (1996) Evaluation of different chemical methods for cross-linking collagen gel, films and sponges. *J Mater Sci Mater M* 7: 215–221.
6. Jayakrishnan A, Jameela SR (1996) Glutaraldehyde as a fixative in bioprotheses and drug delivery matrices. *Biomaterials* 17: 471–484.
7. Zuhdi N, Hawley W, Voehl V, et al. (1974) Porcine aortic valves as replacements for human heart valves. *Ann Thorac Surg* 17: 479–491.
8. Bigi A, Cojazzi G, Panzavolta S, et al. (2001) Mechanical and thermal properties of gelatin films at different degrees of glutaraldehyde crosslinking. *Biomaterials* 22: 763–768.
9. Goldstein JD, Tria AJ, Zawadsky JP, et al. (1989) Development of a reconstituted collagen tendon prosthesis—a preliminary implantation study. *J Bone Joint Surg Am* 71: 1183–1191.
10. Damink LHHO, Dijkstra PJ, Vanluyn MJA, et al. (1995) Glutaraldehyde as a cross-linking agent for collagen-based biomaterials. *J Mater Sci Mater M* 6: 460–472.
11. Speer DP, Chvapil M, Eskelson CD, et al. (1980) Biological effects of residual glutaraldehyde in glutaraldehyde-tanned collagen biomaterials. *J Biomed Mater Res* 14: 753–764.
12. Olde DLH, Dijkstra PJ, van Luyn MJ, et al. (1996) Cross-linking of dermal sheep collagen using a water-soluble carbodiimide. *Biomaterials* 17: 765–773.

13. Kato YP, Christiansen DL, Hahn RA, et al. (1989) Mechanical-properties of collagen-fibers-a comparison of reconstituted and rat tail tendon fibers. *Biomaterials* 10: 38–41.
14. Kato YP, Dunn MG, Zawadsky JP, et al. (1991) Regeneration of achilles-tendon with a collagen tendon prosthesis-results of a one-year implantation study. *J Bone Joint Surg Am* 73: 561–574.
15. Everaerts F, Torrianni M, Hendriks M, et al. (2008) Biomechanical properties of carbodiimide crosslinked collagen: influence of the formation of ester crosslinks. *J Biomed Mater Res A* 85A: 547–555.
16. Sung HW, Chang WH, Ma CY, et al. (2003) Crosslinking of biological tissues using genipin and/or carbodiimide. *J Biomed Mater Res A* 64: 427–438.
17. Chang Y, Tsai CC, Liang HC, et al. (2001) Reconstruction of the right ventricular outflow tract with a bovine jugular vein graft fixed with a naturally occurring crosslinking agent (genipin) in a canine model. *J Thorac Cardiovasc Surg* 122: 1208–1218.
18. Huang LLH, Sung HW, Tsai CC, et al. (1998) Biocompatibility study of a biological tissue fixed with a naturally occurring crosslinking reagent. *J Biomed Mater Res* 42: 568–576.
19. Sung HW, Huang RN, Huang LLH, et al. (1998) Feasibility study of a natural crosslinking reagent for biological tissue fixation. *J Biomed Mater Res* 42: 560–567.
20. Sung HW, Liang IL, Chen CN, et al. (2001) Stability of a biological tissue fixed with a naturally occurring crosslinking agent (genipin). *J Biomed Mater Res* 55: 538–546.
21. Hwang YJ, Larsen J, Krasieva TB, et al. (2011) Effect of genipin crosslinking on the optical spectral properties and structures of collagen hydrogels. *ACS Appl Mater Inter* 3: 2579–2584.
22. Koob TJ, Hernandez DJ (2002) Material properties of polymerized NDGA-collagen composite fibers: development of biologically based tendon constructs. *Biomaterials* 23: 203–212.
23. Koob TJ, Hernandez DJ (2003) Mechanical and thermal properties of novel polymerized NDGA-gelatin hydrogels. *Biomaterials* 24: 1285–1292.
24. Koob TJ, Willis TA, Hernandez DJ (2001) Biocompatibility of NDGA-polymerized collagen fibers I. Evaluation of cytotoxicity with tendon fibroblasts in vitro. *J Biomed Mater Res* 56: 31–39.
25. Koob TJ, Willis TA, Qiu YS, et al. (2001) Biocompatibility of NDGA-polymerized collagen fibers II. Attachment, proliferation, and migration of tendon fibroblasts in vitro. *J Biomed Mater Res* 56: 40–48.
26. Qiu Y, Lei J, Koob TJ, et al. (2014) Cyclic tension promotes fibroblastic differentiation of human MSCs cultured on collagen-fibre scaffolds. *J Tissue Eng Regen M* 10: 989–999.
27. Lu JM, Nurko J, Weakley SM, et al. (2010) Molecular mechanisms and clinical applications of nordihydroguaiaretic acid (NDGA) and its derivatives: an update. *Med Sci Monit* 16: RA93–100.
28. Fisher AA, Labenski MT, Malladi S, et al. (2007) Quinone electrophiles selectively adduct “electrophile binding motifs” within cytochrome c†. *Biochemistry* 46: 11090–11100.
29. Labenski MT, Fisher AA, Lo HH, et al. (2009) Protein electrophile-binding motifs: lysine-rich proteins are preferential targets of quinones. *Drug Metab Dispos* 37: 1211–1218.
30. Moussy Y, Guegan E, Davis T, et al. (2007) Transport characteristics of a novel local drug delivery system using nordihydroguaiaretic acid (NDGA)-polymerized collagen fibers. *Biotechnol Prog* 23: 990–994.

31. Xu B, Chow MJ, Zhang Y (2011) Experimental and modeling study of collagen scaffolds with the effects of crosslinking and fiber alignment. *Int J Biomater* 2011: 172389–172400.
32. Ju YM, Yu B, Koob TJ, et al. (2008) A novel porous collagen scaffold around an implantable biosensor for improving biocompatibility I. In vitro/in vivo stability of the scaffold and in vitro sensitivity of the glucose sensor with scaffold. *J Biomed Mater Res A* 87: 136–146.
33. Baker BM, Mauck RL (2007) The effect of nanofiber alignment on the maturation of engineered meniscus constructs. *Biomaterials* 28: 1967–1977.
34. Elineni KK, Gallant ND (2011) Regulation of cell adhesion strength by peripheral focal adhesion distribution. *Biophys J* 101: 2903–2911.
35. Gallant ND, Michael KE, Garcia AJ (2005) Cell adhesion strengthening: contributions of adhesive area, integrin binding, and focal adhesion assembly. *Mol Biol Cell* 16: 4329–4340.
36. Garcia AJ, Gallant ND (2003) Stick and grip: measurement systems and quantitative analyses of integrin-mediated cell adhesion strength. *Cell Biochem Biophys* 39: 61–73.
37. Kennedy SB, Washburn NR, Simon CG Jr., et al. (2006) Combinatorial screen of the effect of surface energy on fibronectin-mediated osteoblast adhesion, spreading and proliferation. *Biomaterials* 27: 3817–3824.
38. Elliott JT, Tona A, Plant AL (2003) Comparison of reagents for shape analysis of fixed cells by automated fluorescence microscopy. *Cytometry A* 52: 90–100.
39. Zohrabian VM, Forzani B, Chau ZL, et al. (2009) Rho/ROCK and MAPK Signaling pathways are involved in glioblastoma cell migration and proliferation. *Anticancer Res* 29: 119–123.
40. Berens ME, Beaudry C (2004) Radial monolayer cell migration assay. *Methods Mol Med* 88: 219–224.
41. Pratt BM, Harris AS, Morrow JS, et al. (1984) Mechanisms of cytoskeletal regulation. Modulation of aortic endothelial cell spectrin by the extracellular matrix. *Am J pathol* 117: 349–354.
42. Kondo H, Matsuda R, Yonezawa Y (1993) Autonomous migration of human fetal skin fibroblasts into a denuded area in a cell monolayer is mediated by basic fibroblast growth factor and collagen. *In Vitro Cell Dev Biol Anim* 29: 929–935.
43. Tomasz M (1995) Mitomycin C: small, fast and deadly (but very selective). *Chem Biol* 2: 575–579.
44. Kark LR, Karp JM, Davies JE (2006) Platelet releasate increases the proliferation and migration of bone marrow-derived cells cultured under osteogenic conditions. *Clin Oral Implants Res* 17: 321–327.
45. Albarran G, Boggess W, Rassolov V, et al. (2010) Absorption spectrum, mass spectrometric properties, and electronic structure of 1,2-benzoquinone. *J Phys Chem A* 114: 7470–7478.
46. Hamann JN, Tuzek F (2014) New catalytic model systems of tyrosinase: fine tuning of the reactivity with pyrazole-based N-donor ligands. *Chem Commun* 50: 2298–2300.
47. Buxboim A, Rajagopal K, Brown AE, et al. (2010) How deeply cells feel: methods for thin gels. *J Phys Condens Matter* 22: 194116–194125.
48. Engler A, Bacakova L, Newman C, et al. (2004) Substrate compliance versus ligand density in cell on gel responses. *Biophys J* 86: 617–628.

49. Engler AJ, Sen S, Sweeney HL, et al. (2006) Matrix elasticity directs stem cell lineage specification. *Cell* 126: 677–689.
50. Lo CM, Wang HB, Dembo M, et al. (2000) Cell movement is guided by the rigidity of the substrate. *Biophys J* 79: 144–152.
51. Cavalcanti AEA, Volberg T, Micoulet A, et al. (2007) Cell spreading and focal adhesion dynamics are regulated by spacing of integrin ligands. *Biophys J* 92: 2964–2974.
52. Selhuber UC, Erdmann T, Lopez GM, et al. (2010) Cell adhesion strength is controlled by intermolecular spacing of adhesion receptors. *Biophys J* 98: 543–551.
53. Maheshwari G, Brown G, Lauffenburger DA, et al. (2000) Cell adhesion and motility depend on nanoscale RGD clustering. *J Cell Sci* 113: 1677–1686.
54. Massia SP, Hubbell JA (1991) An RGD spacing of 440 nm is sufficient for integrin alpha V beta 3-mediated fibroblast spreading and 140 nm for focal contact and stress fiber formation. *J Cell Biol* 114: 1089–1100.
55. Reyes CD, Garcia AJ (2003) A centrifugation cell adhesion assay for high-throughput screening of biomaterial surfaces. *J Biomed Mater Res* 67: 328–333.
56. Garcia AJ, Huber F, Boettiger D (1998) Force required to break alpha5beta1 integrin-fibronectin bonds in intact adherent cells is sensitive to integrin activation state. *J Biol Chem* 273: 10988–10993.
57. Grover CN, Gwynne JH, Pugh N, et al. (2012) Crosslinking and composition influence the surface properties, mechanical stiffness and cell reactivity of collagen-based films. *Acta Biomater* 8: 3080–3090.



AIMS Press

© 2017 Nathan D. Gallant, et al., licensee AIMS Press. This is an open access article distributed under the terms of the Creative Commons Attribution License (<http://creativecommons.org/licenses/by/4.0>)